A&A 538, A62 (2012)
DOI: 10.1051/0004-6361/201118005

Astronomy & Astrophysics

Shear and vortex motions in a forming sunspot

Twist relaxation in magnetic flux ropes

N. Bello González[1], F. Kneer[2], and R. Schlichenmaier[1]

[1] Kiepenheuer-Institut für Sonnenphysik, Schöneckstr. 6, 79104 Freiburg, Germany
e-mail: [nbello;schliche]@kis.uni-freiburg.de
[2] Institut für Astrophysik, Friedrich-Hund-Platz 1, 37077 Göttingen, Germany
e-mail: kneer@astro.physik.uni-goettingen.de

Received 2 September 2011 / Accepted 28 October 2011

ABSTRACT

Aims. We measure proper motions of fine structures in a forming sunspot to infer information about the dynamics of flux emergence at the sub-photospheric level.
Methods. The active region NOAA 11024 was observed with the Vacuum Tower Telescope at Observatorio del Teide/Tenerife over several days in July 2009. Here, we concentrate on a two-hour sequence taken on July 4, when the leading spot was at an early stage of its evolution. Speckle reconstructions from Ca II K images and polarimetric data in Fe I λ6173 allow us to study proper motions of umbral fine structures.
Results. We detect three prominent features: (1) A light bridge, divided by a dark lane along its axis, shows proper motions in opposing directions on its sides, with velocities of ∼100–500 m s^{-1}. The flows are seen in both the Ca II K and the broadband time sequences. (2) Umbral dots in one umbral region outline a vortex with speeds of up to 550 m s^{-1}. The direction of the motion of the umbral dots is different from that in the light bridge. (3) At one rim of the umbra, the fine structure of the magnetic field moves horizontally with typical velocities of 250–300 m s^{-1}, prior to the formation of the penumbra.
Conclusions. We report on shear and vortex motions in a forming sunspot and interpret them as tracers of twist relaxation in magnetic flux ropes. We suggest that the forming sunspot contains detached magnetic flux ropes that emerge at the surface with different amounts of twist. As they merge to form a sunspot, they untwist giving rise to the observed shear and vortex motions.

Key words. techniques: spectroscopic – Sun: activity – sunspots – techniques: high angular resolution

1. Introduction

The observational properties of fine structures in sunspots remain one of the focci of solar physics research, since they are thought to be the key to understanding the physics of sunspots. In the present study, we report on proper motions of small-scale features in the umbra and a light bridge of a sunspot at its early stage of formation, and we discuss how these motions can be related to the evolution of magnetic flux ropes and their reorganisation during their emergence from the convection zone.

Parker (1979) suggested that the sunspot magnetic field divides into many separate tubes approximately 1 Mm below the photosphere. The bright umbral dots (UDs) and light bridges (LBs), might then represent the occasional upward intrusion of the field-free gas between the flux tubes to the surface. Schüssler & Vögler (2006) carried out realistic three-dimensional magnetohydrodynamic simulations of a plasma that is representative of sunspot umbrae. The simulations of magneto-convection in a monolithic magnetic field reaching 1.2 Mm below the surface produced UDs that are very similar to those observed in terms of brightness, size, and lifetime. Numerical simulations of the formation of an active region were performed by, e.g., Cheung et al. (2010, see also their references to other work). They allowed a vertical semi-torus of a twisted magnetic flux rope to advect into their simulation box reaching 7.5 Mm below the solar surface and studied the evolution during emergence. In the course of its rise, the flux rope expands and splits into many flux tubes that emerge through the surface in a large patch. Later on, the tubes combine to form two spots of opposite polarity that rotate owing to the field twist. Remnants of hot gas with strongly reduced field strength between the re-combined flux tubes are seen as LBs at the surface.

Riethmüller et al. (2008) carried out a detailed observational study of the morphology, evolution, and substructures of UDs. They find proper motions of UDs mainly from the umbral border inward with typical velocities of 420 m s^{-1} and preferred motions of UDs away from an LB on one side and towards the LB on the other side. Watanabe et al. (2010) detected a UD that moved rapidly, with 1.3 km s^{-1}, towards the umbra centre. Sobotka & Puschmann (2009) also found motions of UDs, directed either into the umbra or *along* a faint LB. In addition, these authors, as well as Ortiz et al. (2010) from spectropolarimetric observations, confirm with high spatial resolution data, the existence of dark lanes within UDs, as predicted by Schüssler & Vögler (2006).

Further measurements of proper motions of bright structures in LBs in a pore were performed by Hirzberger et al. (2002). They found irregular motions of grains with velocities of up to 1.5 km s^{-1}. Although they did not discuss this, persistent flows of about half-hour duration can be seen in their Fig. 8. Berger & Berdyugina (2003) presented unidirectional flows of small-scale grains in an LB with an average speed of 900 m s^{-1}. And Rimmele (2008), using a local correlation tracking algorithm, measured proper motions in an LB with speeds of up to

580 m s^{-1}. This flow persists for at least 24 h. Rimmele noted that "the flow vectors indicate that the flow ends in a vortex" and pointed towards a local mechanism as the possible driver of the observed horizontal flows.

2. Observations and data analysis

Our data stem from observations of the active region (AR) NOAA 11024 during July 1–10, 2009 with the Vacuum Tower Telescope at Observatorio del Teide/Tenerife. Schlichenmaier et al. (2010a,b) and Rezaei et al. (2012) described the observational details and reported on the evolution of the AR, on the formation of the spot and on its magnetic properties.

We concentrated on a 1 h 53 min time series, from 08:31 UT to 10:24 UT on July 4, 2009, i.e., during the early stages of the evolution of the AR leading sunspot. Its position on the Sun was 6°E, 25°S, $\cos\theta = 0.88$, with heliocentric angle θ. The data used consisted of: (1) Ca II K bursts taken through a filter with *FWHM* 1 nm; (2) simultaneous speckle observations in Fe I λ6173 (Landé factor $g = 2.5$) with the two-dimensional "Göttingen" Fabry-Perot spectrometer (GFPI, since fall 2009 GREGOR FPI) with its full Stokes polarimetric capability (Bendlin et al. 1992; Puschmann et al. 2006; Bello González & Kneer 2008). Together with the FPI narrow-band frames, broadband burst observations around 6300 Å (*FWHM* 50 Å) were taken.

The Ca II K frames were reconstructed with the speckle interferometry package KISIP (Wöger et al. 2008). The FPI observations were reconstructed with the Göttingen speckle code (de Boer 1996; Janssen 2003; Bello González et al. 2007). The Stokes measurements were demodulated to yield the profiles $(I_\lambda, Q_\lambda, U_\lambda, V_\lambda)$ over the field of view (FOV) as described in Rezaei et al. (2012).

For the present purposes, we used the Ca II K time sequence, the broadband sequence, and the line-of-sight (LOS) component of the magnetic field $B_{\rm LOS}$. The latter was determined from the differences of the centre-of-gravity positions (COG, Rees & Semel 1979) of the $\frac{1}{2}(I + V)$ and $\frac{1}{2}(I - V)$ profiles. Here, the lower 80% of each profile from line minimum to continuum was considered to determine the COG positions.

The sequences were destretched with running means over 11 consecutive images as references. Small remaining drifts were eliminated manually via visual control. The observations had occasionally been interrupted for one time step or longer. The missing images were interpolated linearly from the observations nearest in time. The regular time step was 56–57 s long. Owing to these interruptions, the time step increased occasionally to 59–60 s and to 65–66 s. No correction for parasitic light was applied to Ca II K and broadband images. However, we did not expect parasitic light to influence the positions of bright structures in the umbra nor their proper motions.

3. Results

Figure 1 shows the sunspot under study and its surroundings as seen in Ca II K at 08:37 UT. The image is rotated counterclockwise by ~150° with respect to solar coordinates. At this stage, we could clearly see that the LBs with their dividing dark lanes are remarkable and that the penumbra had developed only rudimentarily (Schlichenmaier et al. 2010a,b). We note without providing additional evidence that the Fe I λ6173 line-minimum images, although of lower spatial resolution, look very similar to the Ca II K images.

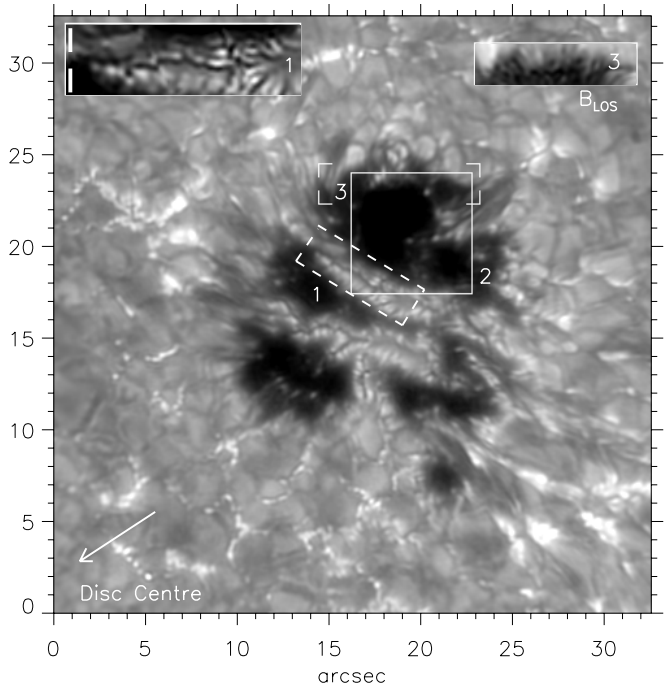

Fig. 1. Leading spot of NOAA 11024 observed on July 4, 2009, 08:37 UT through the Ca II *K* filter with *FWHM* 1 nm. Rectangle "1": part of the light bridge where shear motions are found; the inset '1' shows this LB area rotated to the horizontal and expanded by a factor of two. The vertical white bars in the inset represent the spatial extension selected to create the space-time slices shown in Fig. 2; rectangle "2": part of umbra where umbral dots (UDs) were tracked; rectangle "3" (only corners marked): upper umbral border for space-time slices of the line-of-sight component of the magnetic field, $B_{\rm LOS}$. The latter also from 08:37 UT is shown in the inset "3" (dark meaning the main polarity of the sunspot $B_{\rm LOS}$).

Our study is focused on three different horizontal motions observed in the upper half of the forming spot: (1) In the upper light bridge (rectangle "1" and upper left inset of Fig. 1), shear motions are found; (2) in the largest umbral core of the spot (rectangle "2" of Fig. 1), we observe a clockwise vortex outlined by proper motions of UDs; and (3) at the upper umbral border, in rectangle "3", $B_{\rm LOS}$ exhibits fast horizontal motions.

3.1. Shear motions along a light bridge

Figure 2 presents space-time slices of the section of the LB shown in the left inset of Fig. 1. Since the LB is divided by its central dark lane, we refer to its "upper" and "lower" half in the analysis of horizontal motions. The left two panels of Fig. 2 correspond to Ca II K images, and the right two panels to broadband images. The evolution of the LB lower half is represented by *a* and *c*, and the LB upper half by *b* and *d*. The *x* coordinate lies along the LB. The slices were compressed in the direction perpendicular to *x* for a clear display of the evolution of the moving features. We assumed that the motions occurred parallel to the solar surface and corrected for foreshortening, caused by projection effects.

From the slopes of the structures that are persistent in time, we detected in the lower half of the LB section (panel *a*), motions outwards[1] the spot with velocities of ~100 m s^{-1} (see example

[1] With "outwards", we refer to the direction towards the spot boundary, i.e., towards the upper left in Fig. 1.

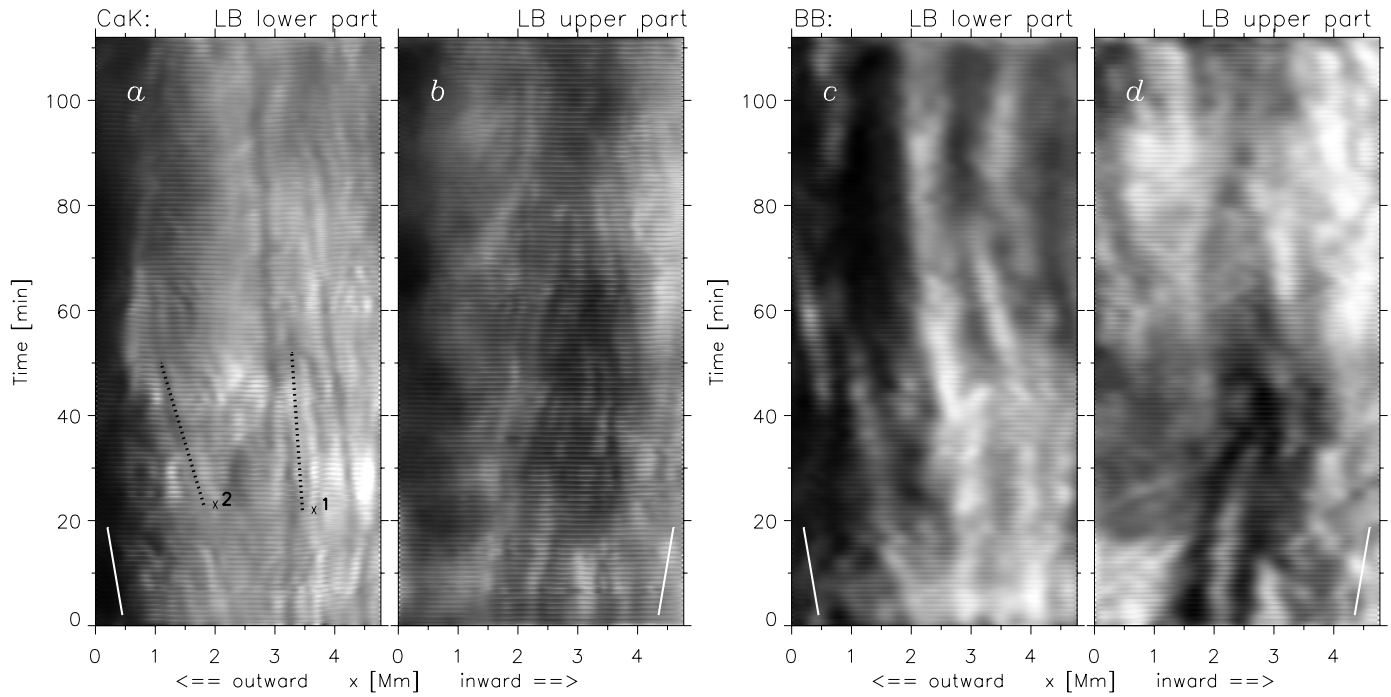

Fig. 2. Space-time slices showing proper motions in the LB section shown in the upper left inset of Fig. 1, corrected for foreshortening; *a* and *b* from the Ca II K images, *c* and *d* from broadband images; *a* and *c* from the LB part below the dark lane seen in Ca; *b* and *d* from the part above the dark lane. The abscissa *x* lies parallel to the LB. Perpendicular to *x*, widths of the slices of 0.″92 for Ca II K and 0.″35 for broadband were chosen, and the slices were compressed appropriately. Discontinuous lines (1 and 2) in panel *a* mark the slope of the trajectory of bright features moving (starting point marked with "x") with speeds of 100 m s^{-1} and 400 m s^{-1}, respectively. For comparison, the slope of the continuous lines refers to 250 m s^{-1}. Ordinate is elapsed time since start of observation.

"1" in Fig. 2) up to 500 m s^{-1} (see example "2" in Fig. 2). In its upper half, the LB displayed proper motions directed mainly inwards the spot, with speeds of ∼250 m s^{-1}. The rightmost 1–1.5 Mm of this part moves outward for ∼30 min starting at time 60 min (since start of the observation, i.e., UT 08:31). The motions stop after 90–100 min. The fine structures have a different appearance in broadband and in Ca II K for two reasons: 1) they are formed in different atmospheric layers; and 2) the resolution in the Ca II K images is higher than in the broadband images. Yet, the flow pattern, i.e., the direction of the propagation and the slopes in Fig. 2 are very similar in the Ca II K and broadband images. These motions can also be discerned in the G-band and Ca II K animations by Schlichenmaier et al. (2010a).

Other parts of the LB and other LBs in this sunspot also exhibit coherent motions at either side of the central dark lane, sometimes also in opposite directions. Nevertheless, these motions are never as persistent as the ones presented in Fig. 2.

3.2. Vortex outlined by proper motions of umbral dots

We present in Fig. 3 the tracks of 62 umbral dots (UDs), which appeared and faded away, in the rectangle "2" of Fig. 1. We refer also to the animations by Schlichenmaier et al. (2010a). The (x, y) positions were marked manually in the broadband images, and only each second position in time, i.e., at intervals of ∼113 s, and occasionally, ∼119 s and ∼131 s, owing to interruptions (see Sect. 2). A correction for foreshortening was also applied. After interpolation from the original pixel distance (0.″112) to a distance half as long (0.″056 or ∼40 km on the Sun), the positions of the UDs intensity maxima could be determined to within a half of this distance. We thus estimated a conservative accuracy of the UDs positions of ±30 km. The tracks were boxcar-smoothed over three (double) time steps. They are indicated for the start with an empty circle when the UDs are visible for the first time and end with a filled circle when the UDs are seen for the last time during the sequence. The lengths of the tracks thus depend on both the speed of proper motion and the life time of the UDs. Some of the tracks are drawn as dotted lines for clarity. The dashed arrows indicate grossly the direction of the motion.

Some of the UD proper motions on the right side of Fig. 3 may stem from intrusions of penumbral grains and peripheral UDs towards the inner umbra. Nevertheless, the motions on the lower, left middle, and upper parts of Fig. 3 occur independently of any penumbral structure and outline a clockwise vortex. Proper-motion velocities range from 40 m s^{-1} to 550 m s^{-1}, with an average of 290 m s^{-1}.

3.3. Proper motions of magnetic field structures

We were able to measure proper motions of the LOS component of the magnetic field, $B_{\rm LOS}$, at the upper umbral border (rectangle "3" in Fig. 1 and upper right inset there). Figure 4 presents space-time slices of $B_{\rm LOS}$ of this part, that are also corrected for foreshortening.

From the beginning of the sequence, structures with strong magnetic fields located at around 3.2 Mm, 4.5 Mm, and 5.5 Mm (see dark features with starting points marked with "x" at the bottom of Fig. 4) show proper motions (typically of 250–300 kms^{-1}) towards the right side. We note that by then in this part of the umbral border, a penumbra had not yet been developed. From ∼45 min (∼UT 09:16) onwards, part of the structures moved towards the left. At 70–80 min, the whole section

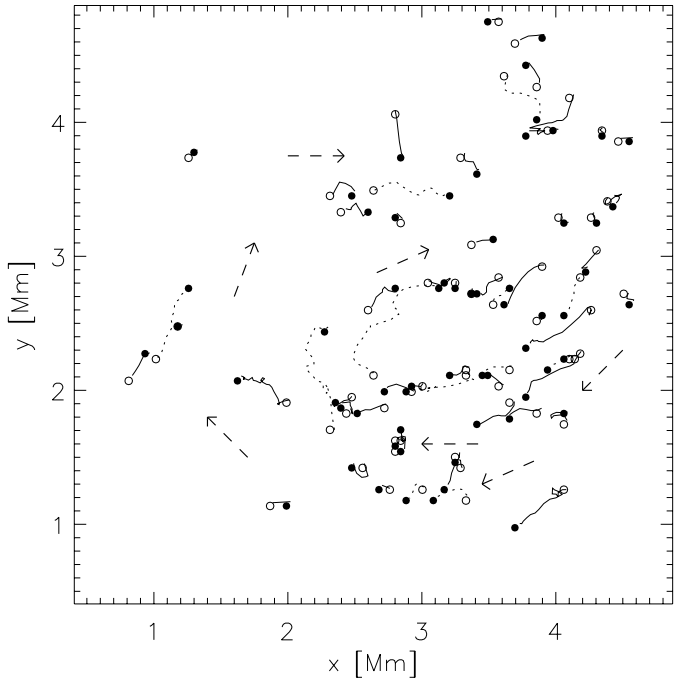

Fig. 3. Tracks of UDs from rectangle "2" in Fig. 1 obtained from the broadband time sequence after correction for foreshortening and boxcar smoothing over three time steps (1 step ~ 113 s, see text). The tracks start with empty circles and end with filled circles. Some of the tracks are drawn as dotted curves for clarity. The dashed arrows indicate grossly the direction of the motions.

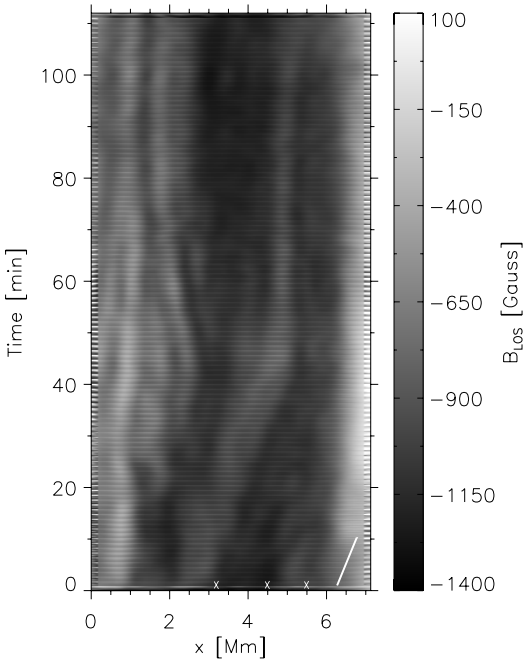

Fig. 4. Space-time slices of line-of-sight component of magnetic field from rectangle "3" in Fig. 1. The abscissa x is parallel to the umbral border, and its scale is corrected for foreshortening. The width of the stripes corresponds to 7.″13. The slices were compressed appropriately. The slope of the white line refers to 250 m s^{-1}. The indicated "x" show the starting position of the features discussed in the text. Ordinate is elapsed time since start of observation.

had come to a rest. At this time, the penumbra had already started to form there (see the online material in Schlichenmaier et al. 2010a).

4. Discussion and conclusion

We have reported on proper motions of small-scale features in a sunspot, during the early stages of its formation. These proper motions are of interest because they hint at the detachment of a rising flux rope into several bundles before emerging at the photospheric level. In Fig. 5, we denote with arrows schematically the location and orientation of these proper motions.

Firstly, we note that we have observed proper motions along a LB (see "1" in Fig. 5). These have been found to be a common feature of LBs (e.g., Berger & Berdyugina 2003; Rimmele 2008). In our case, a section of the LB adjacent to the largest umbral core displays a conspicuous shear motion, i.e., apparent flows in opposite directions on the sides of the central dark lane.

Cheung et al. (2010) found in their numerical simulations that LBs are hot, low-field gas sheets of buoyant material entrained between regions of strong magnetic fields. The different speed and direction of the motions observed in the LB, and the different flow directions of UDs and LB, seen in our data, are not contained in their simulations. Nevertheless, the variation in the flow orientation is similar to the observational finding of Socas-Navarro (2005) on magnetic field torsion, i.e., a gradient in the magnetic field azimuth. From vectorpolarimetry of a complex sunspot, he deduced a strong variation in the torsion including a change of sign.

Secondly, we have measured proper motions of umbral dots (UDs) in the largest umbral core of the spot (circular arrow, "2", in Fig. 5). We note that UD proper motions from 0.4 km s^{-1} to 1.3 km s^{-1} have been reported by several authors

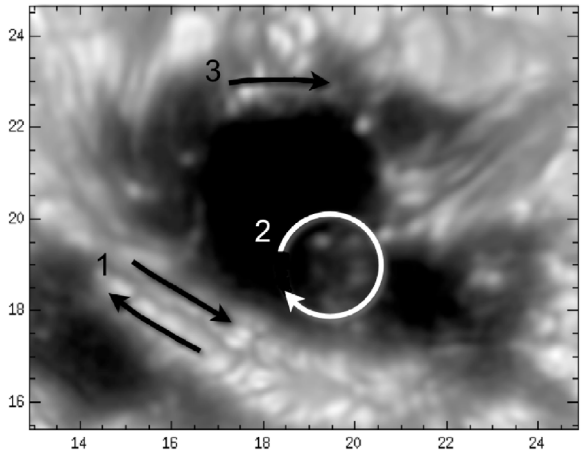

Fig. 5. Graphic summary of the location and orientation of the studied proper motions: (1) shear motions in LBs; (2) vortex motion of UDs; and (3) proper motions of magnetic field structures. Units of a detail from Fig. 1 in arcsec.

(e.g., Riethmüller et al. 2008; Watanabe et al. 2010; Sobotka & Puschmann 2009). They have been found to be aligned mainly towards the umbral centre or along light bridges (LBs). In the sunspot studied here, the umbral dots exhibit a vortex motion during a time span of nearly 2 h, with an average speed of 290 m s^{-1}. We note that this vortex follows a motion that it is the opposite of the LB shear motions. According to the simulations of Schüssler & Vögler (2006), UDs are a phenomenon of magneto-convective nature that originates at least 1.2 Mm below the solar surface.

We thus suggest, that proper motions of UDs are not a surface phenomenon, but rather that UDs are advected by a flow

driven by a process that operates in deeper layers. These motions outline the relaxation of a twist that developed during the rise of the flux tube associated with this part of the umbra. Following Schüssler (1979), Longcope et al. (1996), and Moreno-Insertis & Emonet (1996), these twists are a necessary ingredient for the rise of flux tubes through the convection zone and, as a consequence, for flux emergence to take place.

Finally, we have found that the line-of-sight component of the magnetic field, $B_{\rm LOS}$, exhibits motions parallel to the border of the same umbral core, grossly in the same direction as the vortex outlined by the UDs (see "3" in Fig. 5). We have interpreted this as a signature of the rearrangement of the increasing magnetic flux within the spot (Rezaei et al. 2012, Sect. 5.6), which would be consistent with the measured umbral rotation. However, we note that the motion of the magnetic field halts when the penumbra starts forming at this part of the umbral border.

We point out here four additional properties of the observed sunspot that complement the findings discussed above and help us to understand the formation of sunspots: (1) the sunspot developed from two coalescent individual pores separated by a light bridge (Schlichenmaier et al. 2011); (2) we found no signatures in the spot of an overall rotation that some sunspots do undergo during their evolution (Evershed 1910; Maltby 1964; Nightingale et al. 2000; Brown et al. 2003); instead, the described motions indicate a separate rotation of one part of the spot; (3) the penumbral filaments that formed later *around* the umbral core display a clear curvature (see Rezaei et al. 2012, Sect. 5.3), which is an additional indication of a twisted flux rope in this part of the umbra; and (4) several flares were emitted by this AR during the emergence phase (Valori et al. 2011). Flare energy generation is thought to be favoured by twisting processes in emerging flux ropes (Schrijver et al. 2008; Padinhatteeri & Sankarasubramanian 2010).

We thus suggest the following scenario for the formation of sunspots, which is consistent with the observed vortex and shear motions. The magnetic field of the AR may originate from one thick, deeply rooted flux rope. During its rise through the convection zone, the rope divides into smaller strands. As also suggested by the results of Socas-Navarro (2005) about field torsion, different twists develop for each rope strand owing to the effects of turbulent convective buffeting (Longcope et al. 1998) during the flux rise. When they emerge at the surface, the various strands appear first as small flux tubes as in the Cheung et al. (2010) simulations. The flux tubes then combine to form pores with their own field twists. The pores then coalesce to form sunspots. At this point, pores are components of sunspots but retain their magnetic identity, as well as their own signatures of magnetic twist. The light bridges trapped in-between the regions of strong field either possess their own rotational motion or are entrained by the untwisting of the nearby magnetic fields. Eventually, the LBs disappear upon cooling, the thick rope merges together, and finally a mature umbra with a penumbra forms.

Hence, by means of measuring proper motions in a forming sunspot, we have inferred valuable information that has helped us to understand various aspects of flux emergence and sunspot formation. To achieve this, high spatial resolution observations over an extended period of time (several hours) were mandatory. This was possible thanks to adaptive optics and image reconstruction.

Acknowledgements. We thank R. Cameron and M.C.M. Cheung for helpful and fruitful discussions. N.B.G. acknowledges financial support by Deutsche Forschungsgemeinschaft through grant Schm 1168/9. R.S. acknowledges fruitful discussions within the international team lead by I. N. Kitiashvili on "Filamentary Structure and Dynamics of Solar Magnetic Fields" at ISSI (International Space Science Institute) in Bern. The Vacuum Tower Telescope is operated by the Kiepenheuer-Institut für Sonnenphysik, Freiburg, at the Spanish Observatorio del Teide of the Instituto de Astrofísica de Canarias.

References

Bello González, N., & Kneer, F. 2008, A&A, 480, 265
Bello González, N., Kneer, F., & Puschmann, K. G. 2007, in Modern Solar Facilities – Advanced Solar Science, ed. F. Kneer, K. G. Puschmann, & A. D. Wittmann, Universitätsverlag Göttingen, 217
Bendlin, C., Volkmer, R., & Kneer, F. 1992, A&A, 257, 817
Berger, T. E, & Berdyugina, S. V. 2003, ApJ, 589, L117
Brown, D. S., Nightingale, R. W., Alexander, D., et al. 2003, Sol. Phys., 216, 79
Cheung, M. C. M., Rempel, M., Title, A. M., & Schüssler, M. 2010, ApJ, 720, 233
de Boer, C. R. 1996, A&AS, 120, 195
Evershed, J. 1910, MNRAS, 70, 217
Fan, Y. 2009, ApJ, 697, 1529
Hirzberger, J., Bonet, J. A., Sobotka, M., Vázquez, M., & Hanslmeier, A. 2002, A&A, 383, 275
Janssen, K. 2003, Ph.D. Thesis, Göttingen university
Longcope, D. W., Fisher, G. H., & Arendt, S. 1996, ApJ, 464, 999
Longcope, D. W., Fisher, G. H., & Pevtsov, A. A. 1998, ApJ, 507, 417
Maltby, P. 1964, Astrophys. Nor., 8, 205
Moreno-Inseris, F., & Emonet, T. 1996, ApJ, 472, L53
Nightingale, R. W., Brown, D. S., Shine, R. A., et al. 2000, Eos Trans. AGU, 81, Fall Meeting Suppl., No. SH11A-10
Ortiz, A., Bellot Rubio, L. R., & Rouppe van der Voort, L. 2010, ApJ, 713, 1282
Padinhatteeri, S., & Sankarasubramanian, K. 2010 [arXiv:1010.1082]
Parker, E. N. 1979, ApJ, 230, 905
Puschmann, K. G., Kneer, F., Seelemann, T., & Wittmann, A. D. 2006, A&A, 445, 337
Rees, D. E., & Semel, M. D. 1979, A&A, 74, 1
Rezaei, R., Bello González, N., & Schlichenmaier, R. 2012, A&A, 537, A19
Riethmüller, T. L., Solanki, S. K., Zakharov, V., & Gandorfer, A. 2008, A&A, 492, 233
Rimmele, T. 2008, ApJ, 672, 684
Schlichenmaier, R., Rezaei, R., Bello González, N., & Waldmann, T. A. 2010a, A&A, 512, L1
Schlichenmaier, R., Bello González, N., Rezaei, R., & Waldmann, T. A. 2010b, Astron. Nachr., 331, 563
Schlichenmaier, R., Rezaei, R., & Bello González, N. 2011 [arXiv:1102.0965]
Schüssler, M. 1979, A&A, 71, 79
Schüssler, M., & Vögler, A. 2006, ApJ, 641, L73
Schrijver, C. J., De Rosa, M. L., Metcalf, T., et al. 2008, ApJ, 675, 1637
Sobotka, M., & Puschmann, K. 2009, A&A, 504, 575
Socas-Navarro, H. 2005, ApJ, 631, L167
Valori, G., Green, L.M., Démoulin, P., et al. 2011, Sol. Phys., submitted
Von der Lühe, O., Soltau, D., Berkefeld, T., & Schelenz, T. 2003, SPIE, 4853, 187
Watanabe, H., Tritschler, A., Kitai, R., & Ichimoto, K. 2010, Sol. Phys., 266, 5
Wöger, F., von der Lühe, O., & Reardon, K. 2008, A&A, 488, 375